



Study of Carbon Steel by Mechanical Spectroscopy beyond the Old Limitations

Shimotomai M*

Abstract

A new aspect of carbon precipitates in steel is disclosed by mechanical spectroscopy. The method was applied to the study of carbide precipitation in quench-aged Fe-C alloys, mild steel, and pearlitic steel. Measurements carried out at constant temperature below room temperature (RT) down to -55°C have revealed a new broad peak (NBP) different from neither the Snoek nor the Snoek-Köster peaks. This peak is characterized by the Debye peak with a distribution in relaxation time. The Arrhenius plot yields a large activation energy and gigantic pre-exponential factor. The intensity of NBP increases with aging at temperatures where ϵ -carbide is known to precipitates. It starts to decay at aging time too early for the ϵ -carbide to disappear. NBP is understood by a model of stress-induced reorientation of extra-carbon pairs in ϵ -Fe₃C host lattice. The decay of NBP with aging is accompanied by growth of another peak (NBP'). NBP and NBP' are ascribed to coherent and incoherent ϵ -carbides, respectively. Mechanical spectroscopy has a potential to unravel the unknowns about carbon in steel beyond the old limitations of internal friction measurements at constant frequency. Based on the present findings, the directions for future studies are suggested, which include the precise determination of Fe-C phase diagram with respect to ϵ -carbide, understanding of precipitation hardening in steel and extension of measuring window of mechanical spectroscopy for ϵ -carbide in steel.

Keywords

Mechanical spectroscopy; Steel; Iron-carbon alloy; Epsilon carbide; Precipitation

Introduction

The internal friction Q^{-1} , established in the 1940's, was deemed as a powerful tool for studying the precipitation of carbon atoms in ferrite since the height of the so-called Snoek peak [1], a Debye-type relaxation peak, is proportional to the amount of solute carbon in steel. The method was applied to investigate precipitation kinetics and the solubility of interstitial impurities. The kinetics of precipitation during quench aging of supersaturated solid solutions of carbon and/or nitrogen in iron was studied by Dijkstra [2] and by Wert [3,4]. Early investigations on quench-aged plain Fe-C alloys revealed that the Snoek peak height decreases with aging [2-4]. Doremus [5] studied carbide precipitation between 37 and 170°C in quenched plain Fe-C alloys through the change of the Snoek peak height. Butler [6] found a two-stage loss of carbon from the solid solution of Fe-C alloy.

In those days, measurements of internal friction were carried on highly diffusive elements such as carbon and nitrogen in iron with inverted torsion pendulums as a function of temperature while keeping the frequency constant. Such measurements have several limitations. The measuring temperature interval has to match the temperature of the peak maximum. Moreover, long-range atomic diffusion is not allowed during measurements. Also, the proportionality of the solute content to the peak height is dependent on the texture of the specimens [7]. For accurate analysis the proportionality constant has to be determined individually for each polycrystalline specimen. As regards the practical application of internal friction, steel industry first showed much interest to this method for the control of carbon content during steel sheet production. However, analytical methods such as inductively coupled plasma-atomic emission spectrometry and combustion-infrared absorption method emerged in 1980's. They provided fast, accurate and quantitative analysis of trace carbon in steel and have taken the place of the Snoek peak measurements.

In the last 30 years, mechanical spectroscopy, a frequency-sweep measuring technique for Q^{-1} at fixed temperatures has made progress and gained wide recognition. In this article, novel relaxation peaks found in carbon steel with this method are analyzed. Significance of the finding is discussed in relation to unsolved issues of carbon steel. The discovery of the relaxation peak in Fe-C alloys was preliminarily published in a report on Supermetal Project of Japan [8]. The details and discussion of the investigation with a focus on coherent-incoherent transition are given in reference [9].

Instrumentation

The principle of sub resonance method was briefly given as follows [10]. A specimen is set into forced vibration at a frequency ω low enough compared to the resonance frequency ω_r to permit neglect of the inertial term in the equation of motion. Under the condition $\omega^2 \ll \omega_r^2$ the loss angle φ becomes equal to the phase angle θ between the peak force F_0 and the peak displacement x_0 . From a measurement of φ and the absolute dynamic modulus $|M|$ (proportional to F_0/x_0), the real and imaginary components of the complex modulus may be found. A sub-resonant forced pendulum presents two main advantages [11]. It allows one to perform experiments at very low frequencies and to carry out isothermal measurements as a function of frequency. The sub-resonance method was not widely used for work on crystals due to the difficulty of measuring small phase angles. In 1977, Woigard et al. [12] introduced a torsional pendulum allowing the measurement of internal friction in metals as a function of frequency on a wide range of frequency. With this apparatus they were able to obtain both high and low values of Q^{-1} by phase lag measurements at any frequency between or over 10^{-5} and 10 Hz. The advance of digital technology at that time made the methodology feasible. In addition strong rare-earth magnets such as SmCo₅, Sm₂Co₁₇ and Nd₂Fe₁₄B invented in 1960's~1980's realized powerful twisting of rigid specimens made of metals and alloys.

A mechanical spectrometer, supplied by Vibran Technologies Inc., USA was based on a forced vibration torsion pendulum. It covered five decades in frequency from 10^{-4} to 10 Hz. The strain amplitude during the forced vibration was designed to be kept less than 10^{-5} . Figure 1 shows arrangement of the inverted torsion pendulum. The

*Corresponding author: Shimotomai M, Life member of Japan Institute of Metals and member of The Iron and Steel Institute of Japan, Tel: +81-43-278-9795; E-mail: m-shimotomai@msa.biglobe.ne.jp

Received: June 27, 2017 Accepted: July 11, 2017 Published: July 16, 2017

Peltier effect modules were combined to the spectrometer to make measurements feasible between -40 and 60°C. Helium gas was filled around a specimen as a heat-exchange gas. The temperature of the specimen was kept constant within ± 0.5 K during a scanning over a single sweep of frequency. Circulation of cooling liquid for the Peltier modules accompanied an inevitable mechanical noise. This disturbance determined the lowest limit of measuring frequency at low temperatures. A convection flow of the exchange gas due to temperature gradient along the hanging rod for a specimen limited reliable measurements up to 6 Hz at low temperatures. In case of measurements at as low as -55°C, the cryostat was filled with a freezing mixture of liquid nitrogen and an organic solvent. The specimen in the cryostat naturally warmed up very slowly without any temperature control. The specimen temperature remained roughly constant during a single sweep time of 3 h over 10 Hz to 0.001 Hz. A homogenous magnetic field of 20 mT was applied along a specimen to suppress the magneto-elastic contribution to the damping in iron and steel. Reliable and accurate data were obtained when the torsional rigidity of the specimen was less than the designed value of the instrument. Figure 2 shows the cryostat and solenoid magnet used in the present study.

Results and Discussion

The chemical compositions of specimens are summarized in Table 1. The FeC-1 and FeC-2 specimens were cut from the sheets prepared by carburizing pure iron sheets at 730°C in a flowing mixed gas of CH₄ and H₂. The Steel-A specimen was made of commercial mild steel. The Steel-B specimen was cut from a eutectoid steel sheet. This specimen was beforehand subjected to pearlitic transformation under a magnetic field gradient to attain an excessive carbon concentration in the pearlitic ferrite [13]. The present study started

initially to analyse the enhanced carbon concentration quantitatively by the Snoek peak height. For comparison, a nitrogen-charged specimen, FeN was also prepared. All the specimens were shaped into dimensions similar to those used for tensile testing with spark cutting: the gauge length was 45 mm and the width and thickness were 2-3 mm and 0.7-1.0 mm, respectively.

Relaxation due to epsilon (ε) carbide

New broad peak: The specimen FeC-1, heated to 727°C in vacuum for 0.5 h, was quenched into an oil bath kept at 0°C. The Snoek peak height measured right after the quenching was $3.3 \cdot 10^{-3}$. Two-thirds of the carbon atoms are estimated to be in solution by referring to the chemical analysis (Table 1). The spectra for the FeC-1 specimen aged at 120°C for 1 h are shown in Figure 3. The measurement temperatures were varied between -36°C and -24°C. All the spectra indicate existence of a new broad peak (NBP) in addition to the Snoek peak shown only for the -24°C spectrum for the sake of clarity. The peak maximum is noted to shift to lower frequencies with decreasing temperature. This assures that a thermally activated process is involved in NBP.

Similar measurements were carried out on Steel-A. The specimen was quenched into iced-water subsequent to a solution treatment at 650°C for 30 min. in inert atmosphere. The spectrum taken at RT right after the quenching was dominated by the Snoek peak. Figure 4 shows the spectra for Steel-A at 120°C for 5 h at various temperatures. Here also, the broad peak shifting to lower frequencies with decreasing temperature is noted. The broad maximum is manifested clearly at -34°C and -37°C spectra. Therefore, the existence of NBP, a new hitherto unknown peak of a thermally-activated type, is unquestionable.

Additionally, NBP requires a continuous variation in vibration frequency over three decades to cover the whole profile as shown in Figures 3 and 4. This suggests that the relaxation peak involves a process with a distribution in the relaxation time. The problem of the anelastic process with a distribution of relaxation time was fully analysed by Nowick and Berry [14]. They gave theoretical values in

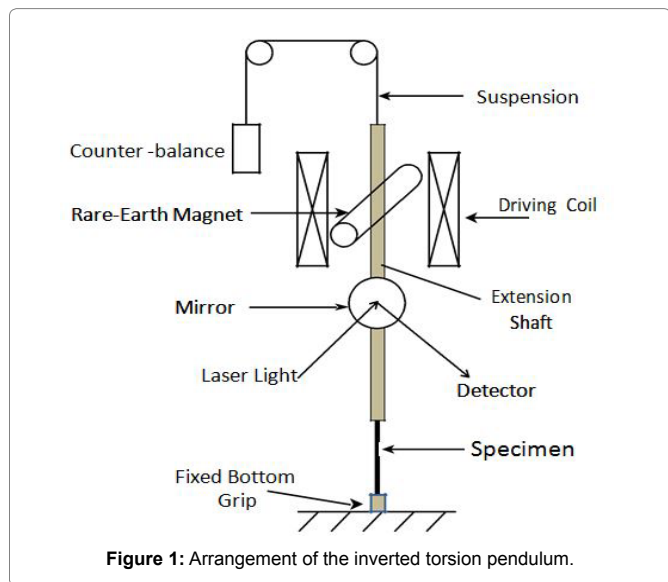


Figure 1: Arrangement of the inverted torsion pendulum.

Table 1: Chemical compositions of specimens (wt. pct).

Specimen	C	N	O	Mn
FeC-1	0.005	0.001	0.003	0.003
FeC-2	0.015	0.001	0.003	0.002
Steel-A	0.038	N.A.	N.A.	0.16
Steel-B	1.00	N.A.	N.A.	~0 (N.A.)
FeN	0.0001	0.013	N.A.	0.002

N.A.: Not Analyzed

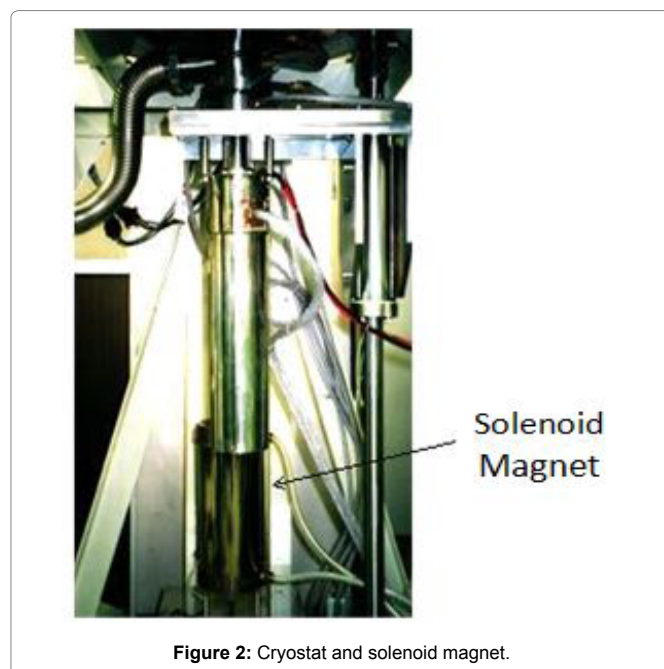


Figure 2: Cryostat and solenoid magnet.

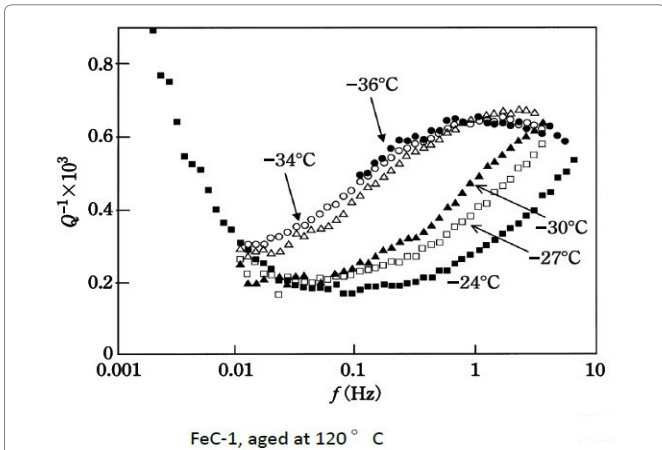


Figure 3: Spectra of FeC-1 measured at various temperatures. The specimen was aged at 120°C for 1 h.

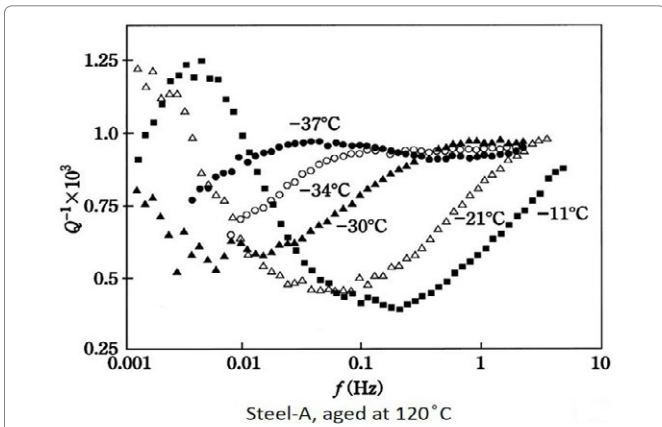


Figure 4: Spectra of Steel-A measured at different temperatures. The specimen was aged at 120°C for 5 h.

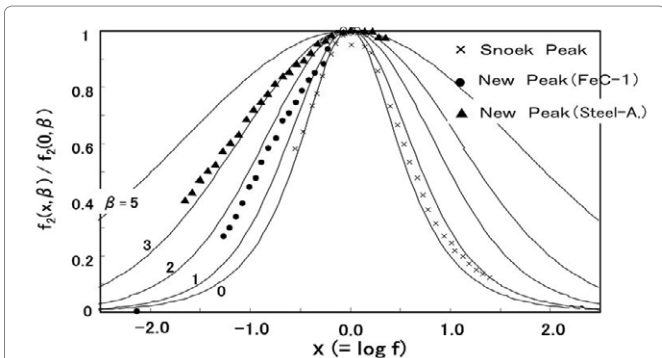


Figure 5: Theoretical relaxation peak curves for various distribution parameters of β . Measured spectra are superimposed.

tabulated form for various distribution parameter β . Figure 5 shows the present spectra superimposed on their theoretical curves. The Snoek peak data taken for Steel-A are close to the $\beta=0$ curve. As for NBP, data for FeC-1 measured at -30°C (refer to Figure 3) are close to the $\beta=2$ curve. Data for Steel-A measured at -30°C (refer to Figure 4) approximately fit to the $\beta=3$ curve. These fittings are regarded as excellent at the left side of NBP. The poor fits on the high-frequency side suggest that another peak might be present at higher frequencies. The -34°C spectrum in Figure 4 is compared with theoretical curve (blue

line) in Figure 6. At high frequencies beyond the peak maximum, the measured data exceed the theoretical values. The difference, shown by the bold broken line, is compared with a thin theoretical curve (black line) assuming $\beta=3$. This plot indicates another peak at higher frequencies. The residue lines evaluated for -37°C and -30°C spectra are also shown in the figure. They are shifted with regard to frequency in a manner which suggests another peak of thermal activation type.

The decay of the Snoek peak and the evolutions of NBP might be studied by aging experiment. A quenched specimen of FeC-1 was subjected to aging treatment which was a combination of step heating and isothermal annealing. Subsequent to every aging step, internal friction measurements were carried out. The interstitial carbon content was monitored by the Snoek peak height measured at RT, while the intensity of NBP was evaluated by its height at 4 Hz taken at -30°C . Their values versus the aging are plotted in Figure 7. The shaded regions in the figure represent isothermal aging treatments. Time scale for the isothermal aging is logarithmic. As for the Snoek peak (left-side ordinate), its height goes down from $3.2 \cdot 10^{-3}$ right after quenching to the minimum value of $3 \cdot 10^{-4}$ after aging at 120°C for 12 h. This behaviour is in agreement with early studies on the aging behavior of Fe-C alloys measured with constant-frequency torsion pendulums [2,3,5]. As regards NBP (right-side ordinate), its growth is closely related with the decline of the Snoek peak up to the aging at 120°C for 3 h. The Snoek peak height begins to recover with aging above 170°C .

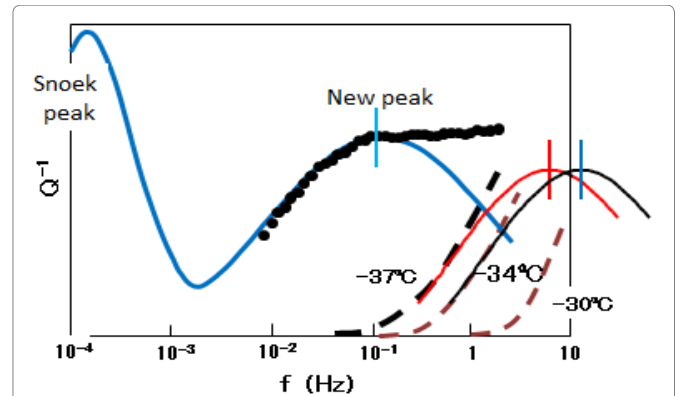


Figure 6: A comparison of the -34°C spectrum of Figure 4 with theoretical curve (blue line). The bold broken line represents the difference between measured and theoretical spectra. Cases for -37°C and -30°C spectra are also shown.

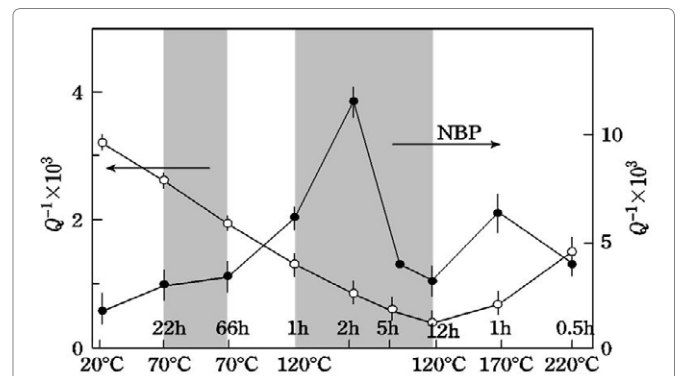


Figure 7: The Snoek peak height at RT (left-side ordinate) and the height of NBP at -30°C (right-side ordinate) versus the evolution of aging treatment for FeC-1. NBP is assumed to have maximum values at 4 Hz. The background values for the peaks have been subtracted.

Early investigations on Fe-C alloys are useful to interpret the present results. Leslie [15] studied the aging behavior of Fe-0.014wt% C alloy quenched from 730°C by means of transmission electron microscopy. He found metastable carbide, now well established as ϵ -carbide, to nucleate above 60°C. The carbide grows appreciably at 100~150°C. This is the just temperature range where a remarkable growth of NBP is observed in Figure 7. Abiko and Kimura [16] carried out detailed studies on the nucleation and evolution of ϵ -carbide in quenched Fe-C alloys by electrical resistivity measurements and also with a transmission electron microscope. One of their conclusions is that the nucleation of ϵ -carbide was mostly completed during the quenching. Both studies lead to an idea that NBP is associated with carbon atoms in ϵ -carbide. Another feature of NBP shown in Figure 7 is that its height decreases sharply by aging beyond 3 h at 120°C. This anomaly might be linked with the previously reported peculiar behavior of ϵ -carbide at prolonged aging time. Doremus [5] found changes in the morphology and structure of precipitate particles to take place at aging stage where nearly all of the solute carbon atoms were drained into the carbide. Abe and Suzuki [17] studied the aging behaviour of low carbon steel by measuring the thermoelectric power and electrical conductivity in the course of aging. They noticed an anomaly in the thermoelectric power vs. conductivity plot at the final stage of aging and conjectured that a coherent-incoherent transition might take place in ϵ -carbide. Thus, present aging study along with literature data strongly suggests that ϵ -carbide is the likeliest model for NBP.

One more peak: To confirm the presence of another peak, measurement was extended to the Steel-B, eutectoid steel. The specimen was fully austenitized at ~870°C and then cooled to 560°C for 2 min for pearlitic transformation under magnetic field gradient before water-quenching. Application of magnetic field gradient during the pearlitic transformation was reported to yield excessive solute carbon atoms in the pearlitic ferrite [13]. Immediately after the quenching, the Snoek peak height measured at RT was 1×10^{-4} . Assuming the pearlite microstructure had equal amounts of ferrite and cementite, the carbon concentration in the pearlitic ferrite was ~0.0002 wt. %. Subsequently, the specimen was aged at 120°C for 0.5 h and set to the cryostat which was then cooled by a freezing mixture of liquid nitrogen and an organic solvent. The measurement started at -55°C. During a single sweep from 10 Hz to 0.001 Hz for 3 h, the specimen was slowly warmed up spontaneously. During repeated sweeps, multiple spectra were accumulated as shown in Figure 8. In the figure two slightly different temperatures are given for each spectrum one for 1 to 0.01 Hz and one for 0.01 to 0.001 Hz. Eight spectra in total are shown in different colours. We start our explanation from the spectrum colored by black, taken at the highest temperature of 12°C. In this spectrum, the left foot of NBP is seen at ~10 Hz. This left foot is manifested stronger with decreasing temperature as seen, for example, in spectra at -16°C. With further decrease of temperature NBP is shifted to lower temperatures. It is important to note that another peak has emerged distinctly on the right side of the spectra taken at -34°C (orange color). Its shape is traced by a dotted theoretical line as a visual aid. This peak also moves to the lower frequencies with decrease of the temperature. Thus, the existence of another peak is confirmed. This peak is denoted as NBP' tentatively. In this specimen the ϵ -carbide is supposed to be precipitated in the pearlitic ferrite, because transmission electron microscopy applied to the similarly heat-treated Fe-1% C-1% Mn and Fe-1% C-0.4% Cr specimens revealed precipitates with diffraction

spots attributable to ϵ - or χ - carbide [13]. To the author's knowledge, χ -carbide is not formed in Fe-C binary alloys.

Coherent-incoherent transition

It has been customary to use the Arrhenius Plot to analyze the activation energy E and pre-exponential factor τ_0^{-1} of a relaxation process. For a thermally activated process with a distribution in relaxation time $\ln \tau_m$, instead of $\ln \tau$, is plotted against $1/T$. Here, the most probable value of τ_m is related to the peak frequency f_{max} by $2\pi f_{max} \tau_m = 1$. If this is plotted on NBPs in FeC-1, FeC-2, Steel-A and Steel-B, as well as on NBP' in Steel-B, this produces straight lines through the data points, as shown in Figure 9. The slope of a line gives the activation energy E while the intercept on the vertical axis yields the pre-exponential factor τ_0^{-1} of the relaxation process. Table 2 summarizes these Arrhenius parameters as well as those obtained for the Snoek peak. NBP and NBP' have enormous values: activation energies about three times that of the Snoek peak, along with large pre-exponential factors as high as that of the Snoek peak cubed.

Note that the very small thermal activation factor is compensated by the gigantic pre-exponential factor for thermal relaxations in NBP and NBP'. This kind of compensation between the activation energy

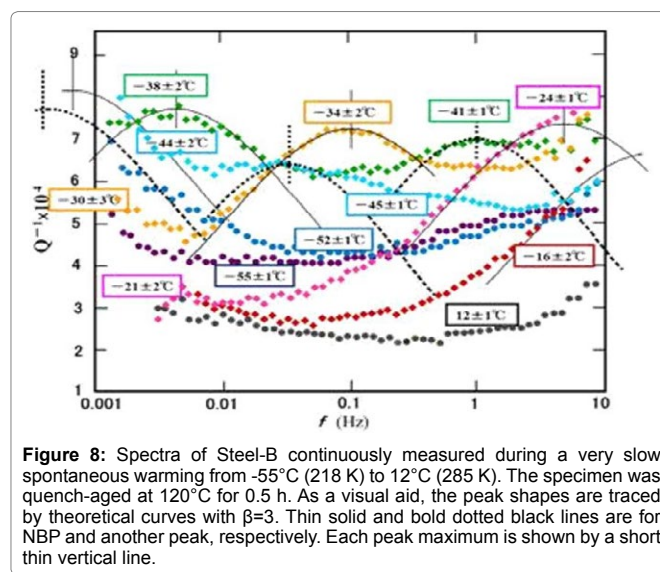


Figure 8: Spectra of Steel-B continuously measured during a very slow spontaneous warming from -55°C (218 K) to 12°C (285 K). The specimen was quench-aged at 120°C for 0.5 h. As a visual aid, the peak shapes are traced by theoretical curves with $\beta=3$. Thin solid and bold dotted black lines are for NBP and another peak, respectively. Each peak maximum is shown by a short thin vertical line.

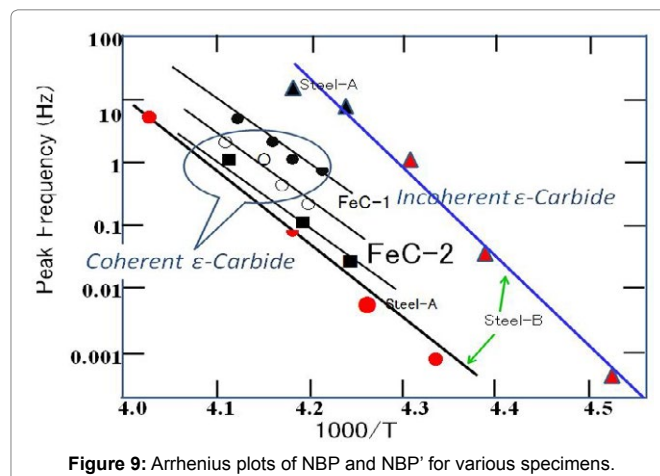


Figure 9: Arrhenius plots of NBP and NBP' for various specimens.

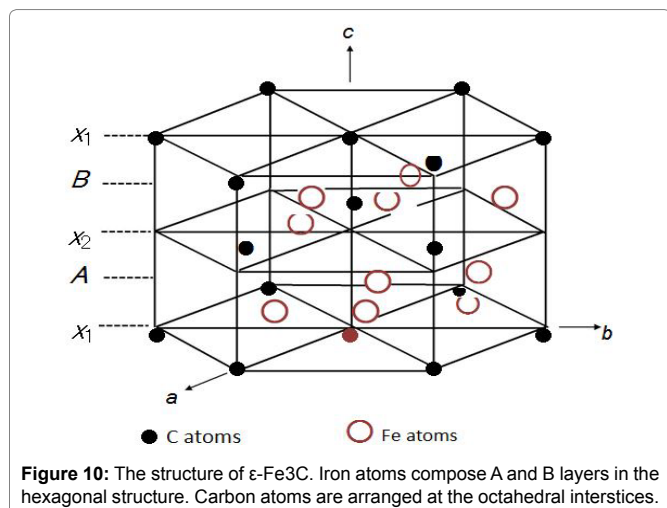
and pre-exponential factor has been observed for diffusion on metallic surfaces [18], for grain boundary internal friction in aluminium [19] in viscosity measurements of glasses [20], and in kinetic studies of catalysis [21,22]. Also, as shown in Figure 9, the points for NBP' in Steel-B (red triangles) and in Steel-A (black triangles) form almost a straight line. This behaviour implies that the local structure around NBP' centers is nearly the same regardless of carbon content. Contrary to this, the parameters of NBP are dependent on the specimens. In fact, the table shows that the activation energy and pre-exponential factor of NBP are increased with carbon concentration. This indicates that a difference in lattice strain influences the values of parameters. Since NBP and NBP' have characteristic features in common, they should be in close relationship. NBP has been ascribed to ϵ -carbide at the end of previous section. This leads to a logical conclusion that NBP are due to coherent ϵ -carbide and NBP' to incoherent one.

The ϵ -carbide model is reasonable in considering the atomic mechanism of the thermal relaxation. Figure 10 depicts the structure of ϵ -Fe₃C, where iron atoms compose A and B layers in the hexagonal structure. Carbon atoms, the small filled circles, are incorporated at the octahedral interstices. Since the composition of real ϵ -carbide has been analysed as Fe_{2.4}C [23-25], extra carbon atoms are allowed to occupy the interstices of the ϵ -Fe₃C structure up to the Fe_{2.4}C composition. Then, the most promising candidates for the relaxation centers are the extra carbon atoms in Fe_{2.4}C. An isolated extra carbon atom in an otherwise perfect hexagonal lattice of ϵ -Fe₃C is unable to undergo stress-induced reorientation due to symmetry requirement. A pair of interstitial carbon atoms could produce a thermal relaxation peak if three successive steps shown in Figure 11 can complete the reorientation of the interstitial carbon pair. The possibility of a pair of substitutional impurity and interstitial carbon are safely ruled out because the relaxation peak was observed also in pure Fe-C alloys. Detailed discussion on the process and kinetics is found elsewhere [9].

Conclusion and Future Studies

Ferritic Steel

Despite the fact that the quench-aging of iron has been exhaustively studied in the past, many aspects of the process remain obscure. The principal unknowns remaining in the quench-aging of iron-carbon alloys are the identification of the metastable carbide, the



nature of matrix nucleation sites, and the mechanism of strengthening by the metastable carbide. These comments were made by Leslie in 1961 [15]. Here, the metastable carbide refers to ϵ -carbide. Since those days, it seems that little progress has been made. A phase diagram of Fe-C system was given in relation to the precipitation of ϵ -carbide by Abiko and Kimura [16]. Their diagram is reproduced in Figure 12 modified with the present results. The blue dotted line denotes the tentative coherent-incoherent transition line. Unsolved issues related to ϵ -carbide include determination of the line of coherent-incoherent transition, the mechanism and kinetics of transfer of Fe_{2.4}C to cementite, the matrix nucleation sites and the role of substitutional

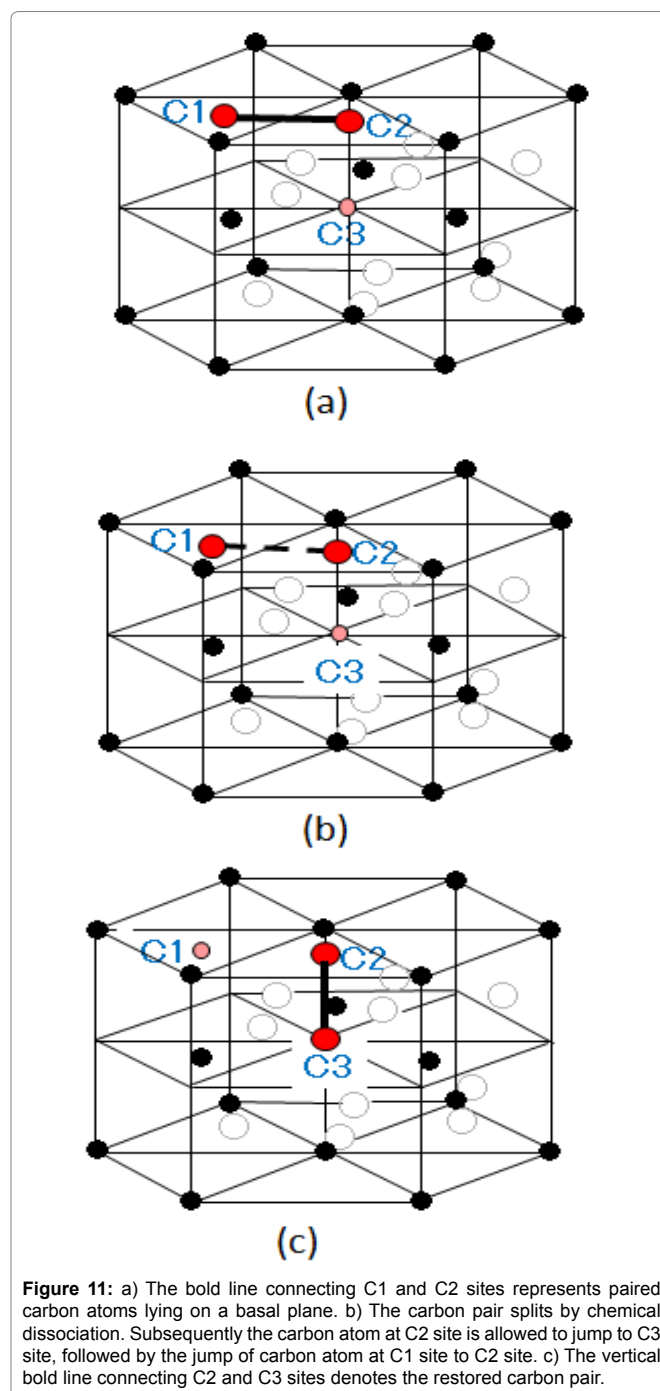


Table 2: Activation Energy E and Pre-exponential Factor τ_0^{-1} of relaxation peaks.

Peak	Specimen	E (kcal/mole)	τ_0^{-1} (s ⁻¹)
NBP (Coherent Carbide)	FeC-1	46 ± 4	10 ⁴⁰ ~10 ⁴⁴
	FeC-2	48 ± 3	10 ⁴² ~10 ⁴⁴
	Steel-A	49 ± 6	10 ³⁷ ~10 ⁴⁸
	Steel-B	53 ± 3	10 ⁴³ ~10 ⁴⁷
NBP' (Incoherent Carbide)	Steel-B	64 ± 6	10 ⁵⁶ ~10 ⁶⁴
Snoek Peak	Steel-A	18.4	5.4 × 10 ¹⁴

impurity atoms. The change of interfacial energy of matrix-carbide upon the coherency loss is also to be determined. Mechanical spectroscopy may be useful to solve the problems.

Martensitic steel

The stages of aging and tempering of ferrous martensite have been studied for years. The first stage of aging involves clustering of carbon atoms in *c*-oriented octahedral sites, while the second stage is associated with a modulated tweed microstructure containing high-carbon regions which may be interpreted as either advanced carbon clusters or coherent ϵ -carbides [26]. In the second stage, ϵ -carbide is precipitated from the retained austenite also. The evolution of ϵ -carbide with tempering was studied by transmission electron microscopy [27]. The unknowns are the nucleation site, the effects of coherency and its loss on the growth kinetics and morphology, the mechanism of the transformation of ϵ -carbide to cementite, and also the role of substitutional impurity atoms. Furthermore, thermodynamic data of ϵ -carbide has not been reported. Thus, the study of ϵ -carbide by mechanical spectroscopy will be valuable in many aspects. The characteristic behaviour of the relaxation peak due to the incoherent ϵ -carbide in martensite would be similar to one discovered in this study. As regards the coherent ϵ -carbide, the behaviour of the ϵ -carbide peak, if exists, is quite unknown because the host crystal structure of martensite is different from the ferrite phase.

Commercial medium-carbon steel

Eglin steel is an ultra-high strength steel alloy that was developed at Eglin Air Force Base in the early 2000s and has since been patented in 2009 [28]. The steel has strength levels similar to AerMet100, AF1410 and HP9-4-30, but at a reduced cost due to a reduction or elimination of expensive alloying elements such as nickel and cobalt. Its typical composition is Fe-0.26C-2.70Cr-0.65Mn-0.42Mo-1.00Ni-1.00Si-1.00W (wt. %). Here, tungsten is contained for keeping ultra-high strength at high temperature needed for military use. More importantly, silicon is added to enhance toughness by retarding cementite formation and to stabilize austenite. Consequently, precipitation of ϵ -carbide is well developed till the formation of cementite, which was evidenced by transmission electron microscopy [28]. This class of steel belongs to medium-carbon steel and could be useful for general use without addition of alloying elements. The influence of ϵ -carbide on the precipitation hardening will be worthy of intense investigation. The dislocation cutting and Orowan looping of ϵ -carbide in relation to coherency loss will be an interesting subject. The potential of precipitation strengthening in medium-carbon steel has not yet been explored.

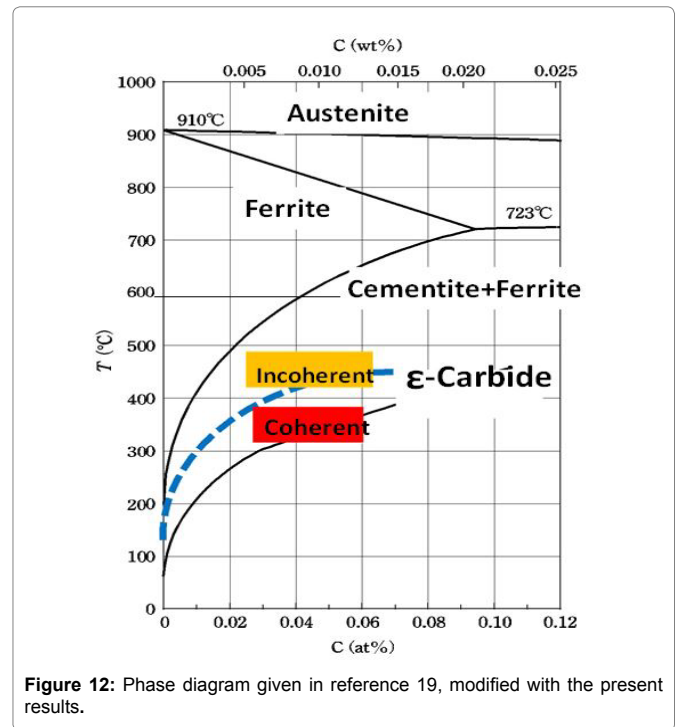


Figure 12: Phase diagram given in reference 19, modified with the present results.

Extension of the measuring window

Internal friction Q^{-1} has been more often measured as a function of temperature. Figure 13 illustrates a simulated spectrum of carbon steel vs. temperature taken at 1 Hz. The figure is composed of the present findings superimposed on a figure given in an article by Kamber et al. [29]. In the past, researchers were so absorbed in the Snoek and Snoek-Köster peaks that the temperature range between -100°C and 0°C were almost neglected. The figure indicates that this range is important for the study of ϵ -carbide. However, this kind of experiment would require some skills. Furthermore, the measurement will be time-consuming. It would be more convenient to adopt the mechanical spectroscopy.

Figure 14 is a modified version of Figure 9. The three straight lines represent Arrhenius plots for the coherent and incoherent ϵ -carbide peaks as well as for the carbon Snoek peak. The blue square denotes a frequency vs. temperature domain which is desirable as a measuring window for the study of aging process in carbon steel by mechanical spectroscopy. With an electronic cooling device, it is easy to cool specimens to as low as -35°C for measurements. A necessary and important modification is the extension of measuring frequency up to several hundred Hertz. This improvement would be realized when a specimen bar is excited in sub-resonant mode with one end of the specimen clamped to a support. In such a configuration, measurements in subresonant mode up to 200 Hz might be possible since the resonant frequency estimated as about 1 kHz, depending on the material and specimen dimensions. Frequently, the mechanical clamp suffers from the disadvantage that it can cause significant losses due to the rubbing friction. To minimize this disadvantage, some authors used specimens with special shape for the mobile part. Mizubayashi et al. successfully measured the Young's modulus of cementite films in a clamped-free mode with a thick end for clamping [30]. The excitation and detection of forced subresonant vibration of the specimen and signal processing will be of central importance. The medium-frequency mechanical

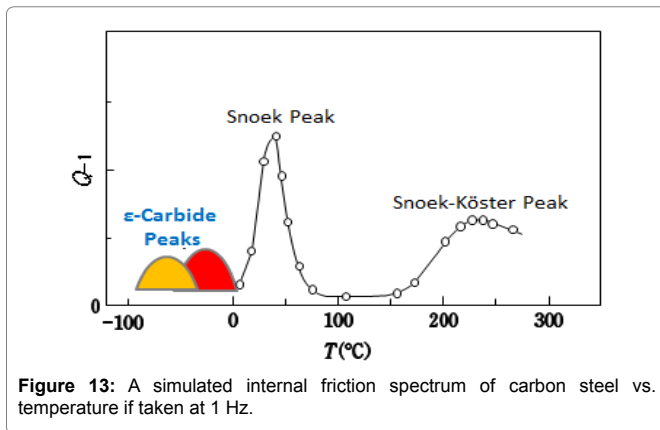


Figure 13: A simulated internal friction spectrum of carbon steel vs. temperature if taken at 1 Hz.

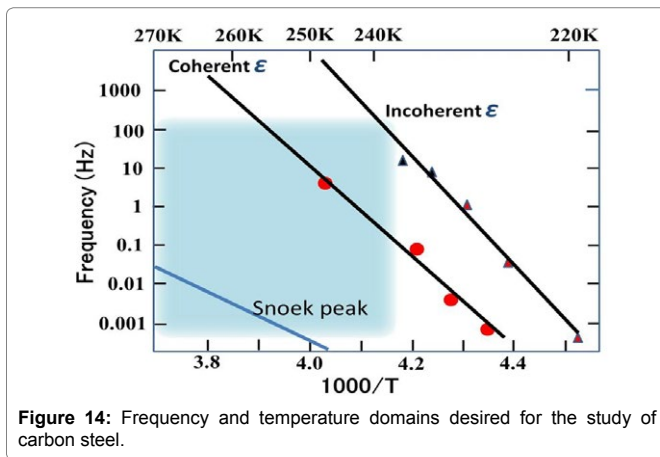


Figure 14: Frequency and temperature domains desired for the study of carbon steel.

spectroscopy proposed here has never been reported before to the author's knowledge. The conditions which must be fulfilled for low-frequency high-resolution mechanical spectroscopy have been fully discussed by Magalas [31]. The requirements will also apply to the medium-frequency case.

Summary

A mechanical spectrometer combined with the Peltier modules was applied to the study of carbide precipitation in quench-aged Fe-C alloys, mild steel, and pearlitic steel. By measuring mechanical loss spectra below RT, a new broad peak (NBP) is revealed. This peak is related to thermal activation and its line shape obeys the equation of the Debye peak with a distribution in relaxation time. The Arrhenius plot yields a large activation energy and gigantic pre-exponential factor. The intensity of NBP grows with aging at temperatures where precipitation of ϵ -carbide has been reported. By isothermal aging at 393 K, the intensity sharply decreases at durations over 3 h. This decay is accompanied by appearance of another similar peak (NBP'), which has a peak frequency two orders higher than that of NBP. NBP and NBP' are ascribed to coherent and incoherent ϵ -carbides, respectively. These peaks are understood assuming reorientations of extra carbon pairs in the ϵ -carbide. Thus, mechanical spectroscopy is powerful in disclosing unknowns in carbon steel. The directions for future studies are suggested, which include the precise determination of Fe-C phase diagram with respect to ϵ -carbide, research on the precipitation hardening in steel and extension of measuring window of mechanical spectroscopy for the sake of practical application of the method.

References

1. Snoek JL (1941) Effect of small quantities of carbon and nitrogen on the elastic and plastic properties of iron. *Physica* 8: 711-733.
2. Dijkstra LJ (1949) Precipitation phenomena in the solid solutions of nitrogen and carbon in alpha iron below the eutectoid temperature. *Trans AIME* 185: 252-260.
3. Wert CA (1949) Precipitation from solid solutions of C and N in α -iron. *J Appl Phys* 20: 943-949.
4. Wert CA (1954) Precipitation out of dual solid solutions of carbon and nitrogen in alpha-iron. *Acta metal* 2: 361-367.
5. Doremus RH (1960) The precipitation of carbon from alpha iron II. Kinetics. *Trans Metall Soc AIME* 218: 596-605.
6. Butler JF (1966) Kinetics of the two-stage precipitation of carbon from ferrite. *J Iron Steel Inst* 204: 127-133.
7. Magalas LB, Fantozzi G, Rubianes J, Malinowski T (1996) Effect of texture on the Snoek relaxation in commercial rolled steel. *J Physique IV* 6: 147-150.
8. Shimotomai M (2002) Report of the Ferrous Super Metal Consortium of Japan. The Japan Research and Development Center for Metals, Tokyo.
9. Shimotomai M (2016) Coherent-incoherent transition of ϵ -carbide in steels found with mechanical spectroscopy. *Metall Mater Trans A* 47A: 1052-1060.
10. Nowick AS, Berry BS (1972) *Anelastic Relaxation in Crystalline Solids*. Academic Press, New York.
11. Rivière A (2001) *Mechanical Spectroscopy Q-1 2001: With Applications to Materials Science*, Trans Tech Pub.
12. Woigard J, Sarrazin Y, Chaumet H (1977) Apparatus for the measurement of internal friction as a function of frequency between 10-5 and 10 Hz. *Rev Sci Instrum.* 48: 1322-1325.
13. Shimotomai M (2003) Influence of magnetic-field gradients on the pearlitic transformation in steels. *Mater Trans JIM* 44: 2524-2528.
14. Nowick AS, Berry BS (1961) Lognormal distribution function for describing anelastic and other relaxation processes. *IBM J Res Develop* 5: 297-320.
15. Leslie WC (1961) The quench-aging of low-carbon iron and iron-manganese alloys: an electron transmission study. *Acta Met* 9: 1004-1022.
16. Abiko K, Kimura H (1976) Nucleation of ϵ -phase precipitates in α -iron. *Trans Japan Inst Metals* 17: 383-392.
17. Abe H, Suzuki T (1980) Thermoelectric power versus electrical conductivity plot for quench-aging of low-carbon aluminium-killed steel. *Trans ISIJ* 20: 690-695.
18. Boisvert G, Lewis LJ, Yelon A (1995) Many-body nature of the Meyer-Nelde compensation law for diffusion. *Phys Rev Lett* 75: 469-472.
19. Jiang WB, Kong QP, Molodov DA, Gottstein G (2009) Compensation effect in grain boundary internal friction. *Acta mater* 57: 3327-3331.
20. Hiki Y (2011) Mechanical relaxation near glass transition studied by various methods. *J Non-Crystalline Solids* 357: 357-366.
21. Kaufman F, Gerri NJ, Pascale DA (1956) Halogen catalyzed decomposition of nitrous oxide. *J Chem Phys* 24: 32-34.
22. Karpinski Z, Gandhi SN, Sachtler WMH (1993) Neopentane Conversion Catalyzed by Pd in L-Zeolite: Effects of Protons, Ions, and Zeolite Structure. *J Catalysis* 141: 337-346.
23. Cohn EM, Hofer LJE (1953) Some thermal reactions of the higher iron carbides. *J Chem Phys* 21: 354-359.
24. Caballero FG, Miller MK, Garcia-Mateo C (2011) Atom probe tomography analysis of precipitation during tempering of nanostructured bainitic steel. *Metall Mater Trans A* 42A: 3660-3668.
25. Song W, Appen J, Choi P, Dronskowski R, Raabe D, et al. (2013) Atomic-scale investigation of ϵ and θ precipitates in bainite in 100Cr6 bearing steel by atom probe tomography and ab initio calculations. *Acta Mater* 61: 7582-7590.

26. Olson GB, Cohen M (1983) Early stages of aging and tempering of ferrous martensites, Metall Trans A 14A: 1057-1065.
27. Ohmori Y, Tamura I (1992) Epsilon carbide precipitation during tempering of plain carbon martensite. Metall Trans A 23A: 2737-2751.
28. Leister BM, Dupont JN, Watanabe M, Abrahams RA (2015) Mechanical properties and microstructural evolution of simulated heat-affected zones in wrought Eglin steel. Metall Mater Trans A 46A: 5727-5746.
29. Kamber K, Keefer D, Wert G (1961) Interactions of interstitials with dislocations in iron. Acta Mater 9: 403-414.
30. Mizubayashi H, Li SJ, Yumoto H, Shimotomai M (1999) Young's modulus of single phase cementite. Scripta Mater 40: 773-777.
31. Magalas LB (2015) Development of high-resolution mechanical spectroscopy, HRMS: status and perspectives. Arch Metall Mater 60: 2069-2076.

Author Affiliation

[Top](#)

Japan Institute of Metals, Japan

Submit your next manuscript and get advantages of SciTechnol submissions

- ❖ 80 Journals
- ❖ 21 Day rapid review process
- ❖ 3000 Editorial team
- ❖ 5 Million readers
- ❖ More than 5000 
- ❖ Quality and quick review processing through Editorial Manager System

Submit your next manuscript at • www.scitechnol.com/submission